Demystifying long-term changes observed by GNSS: comparison with GRACE observations and hydrological models

Jan Mikocki[1], Anna Klos[1], Ozge Gunes[1,2], Artur Lenczuk[1], Janusz Bogusz[1]

Contact e-mail: jan.mikocki@wat.edu.pl

1) Military University of Technology, Warsaw, Poland
2) Yildiz Technical University, Istanbul, Turkey

Direct link to the abstract

EGU General Assembly 2023
Vienna, Austria & Online | 23–28 April 2023

INTRODUCTION

Water is a chemical compound that meets everyone's basic needs. However, extreme changes in water resources may lead to serious economic problems, as well as threaten human life. Monitoring of the variability of water resources in the past was made possible by hydrological models, but nowadays geodetic techniques are also used for this purpose. To carry out our analyses, we used Global Navigation Satellite Systems (GNSS) station displacement time series and displacement time series determined from Gravity Recovery and Climate Experiment (GRACE) observations, as well as from GRACE-assimilating high-resolution hydrological model Global Land Water Storage (GLWS) v2.0 for locations of 1039 GNSS permanent stations distributed around the world. The main goal of our study was assessment of long-term changes derived from the mentioned data sets, as well as comparing them to each other in terms of changes in the terrestrial hydrosphere. At the beginning, we corrected GNSS time series for non-hydrospheric effects to obtain signals caused by the load of water masses. Secondly, we converted GRACE and GLWS time series expressed in equivalent water height (EWH) to vertical displacements using Green's functions to make all three data sets comparable with each other. Moreover, we performed a range of global analyses, based on which we selected time series to show the effectiveness of geodetic techniques in detecting extreme changes in water resources.

DATA

1) A set of 1039 global permanent GNSS network time series processed by the International GNSS Service (IGS) in the form of the latest reprocessing (repro3) and aligned to ITRF2020 reference frame. Data was provided as Software Independent Exchange (SINEX) format files with weekly temporal resolution, covering the period from 2 January 1994 to 31 December 2020 (ftp://igs-rf.ign.fr/pub/repro3). We removed outliers, offsets and predictions of vertical displacements of non-tidal atmospheric and non-tidal oceanic loadings, using models from the German Research Centre for Geosciences (GFZ).
2) Non-tidal atmospheric loading (NTAL) model and non-tidal oceanic loading (NTOL) model, provided by GFZ. Both on a 0.5°x0.5° grid with 3-hour temporal resolution for Center of Mass (CM) Earth's system reference frame, covering the period from 2003 to 2019. We interpolated predictions of vertical displacements from NTAL and NTOL models to coordinates of GNSS stations. Then, we averaged 3-hour solutions to receive monthly temporal resolution, and finally, we subtracted them from GNSS time series (http://rz-vm115.gfz potsdam.de:8080/repository/entry/show?entryid=24aacdfe-f9b0-43b7-b4c4-bdbe51b6671b).
3) GRACE/-FO Center For Space Research (CSR) RL06 v.02 1°x1° monthly mascon solutions, covering the period from January 2003 to December 2019. We didn't subtract any effects, because a combination of non-tidal atmospheric and non-tidal oceanic loadings (GAC product) and bottom-pressure over oceans (GAD product, equal to zero over lands) had already been modelled and removed (https://www2.csr.utexas.edu/grace/RL06_mascons.html).
4) GRACE-assimilating high-resolution GLWS v2.0 global (except from Greenland and Antarctica) hydrological model on a 0.5°x0.5° monthly grid, covering the period from January 2003 to December 2019, provided personally by University of Bonn.

RETRIEVING LONG-TERM SIGNALS

1) We detrended all three datasets of GNSS-observed, GRACE-derived and GLWS-predicted vertical displacements. Then, we used a non-parametric wavelet analysis to derive the long-term components of detrended vertical displacements. We used a Meyer's mother wavelet and decomposed the monthly displacements into four pre-defined timescales. We used the last approximation, which covers all signals with periods above 3.0 years and interpreted them as long-term components.
2) We calculated Pearson linear correlation coefficients between the data sets and the corresponding p-values in order to assess the correlation significance - we assumed a significance level of 0.05.
3) We applied dynamic time warping (DTW) algorithm, the analysis is performed so that the total of the Euclidean distances between the two signals is as small as possible.
4) We computed RMS values to determine the order of magnitude of vertical displacements for all of the data sets.
5) We prepared Lomb-Scargle periodograms in order to examine periodic signals, finding periods of maximum values of power spectral density.
6) We subtracted mean values from all of the time series, so epochs of intersections with horizontal axis (zero point) contain information about the beginning or the end of particular disaster. We compared our results with the international disasters database (EM-DAT - https://www.emdat.be/). We calculated maximum or minimum values, depending on whether these spans represent floods or droughts, as well as corresponding epochs for the mentioned values, rejecting peaks, where values are within the range of ± 2mm for GNSS time series.

COMPARISON OF THE DATA SETS

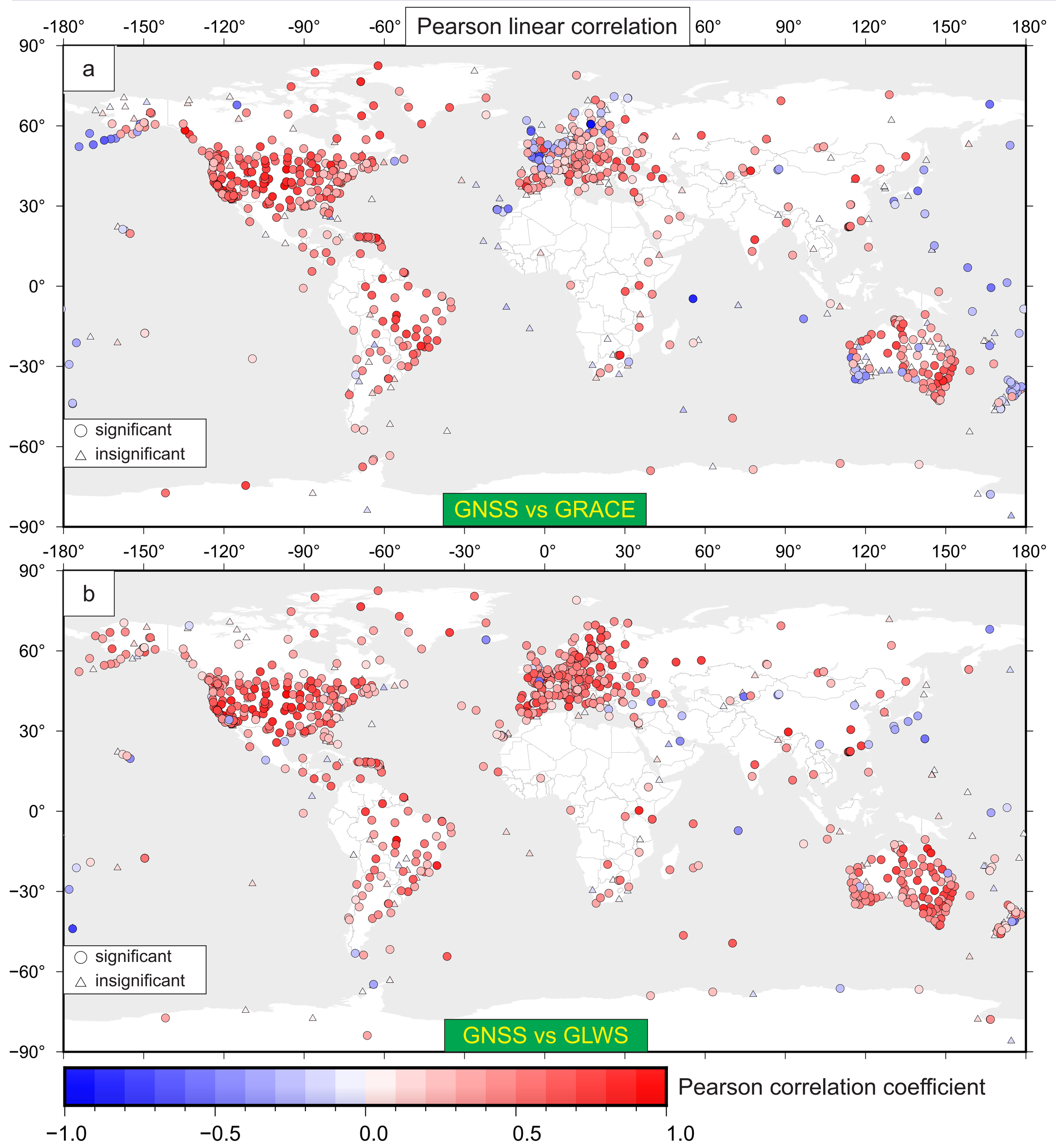

⬆ **Fig. 1.** Pearson correlation coefficients between time series: **a)** GNSS (NTAL/NTOL removal) and GRACE (GAC/GAD removal), **b)** GNSS (NTAL/NTOL removal) and GLWS. GNSS stations marked as circles show significant correlation, and those marked as triangles show insignificant correlation.

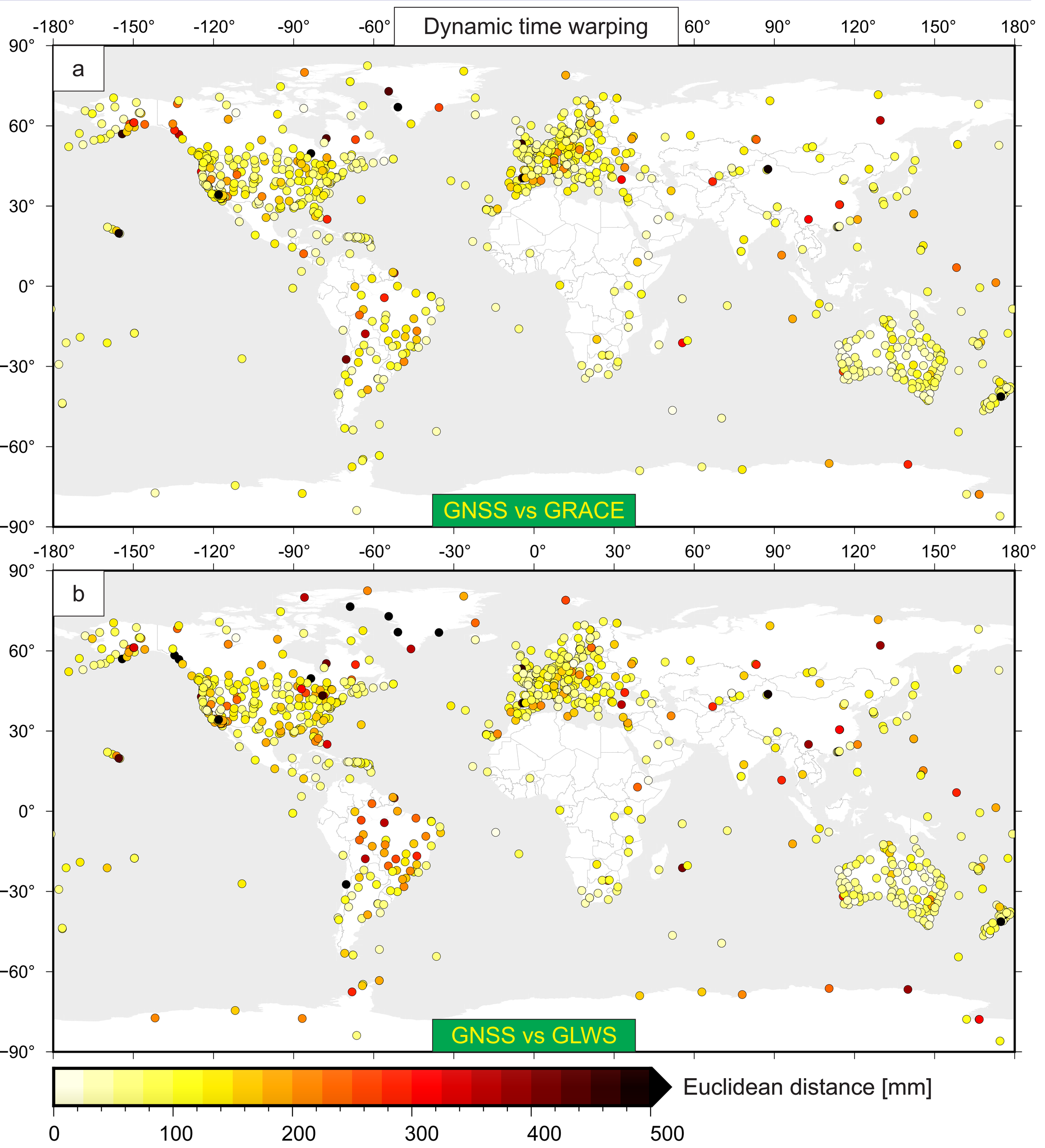

⬆ **Fig. 2.** DTW algorithm - sum of Euclidean distances (mm) between time series: **a)** GNSS (NTAL/NTOL removal) and GRACE (GAC/GAD removal), **b)** GNSS (NTAL/NTOL removal) and GLWS.

IMPACT OF NTAL AND NTOL ON GNSS VS GRACE COMPARISON

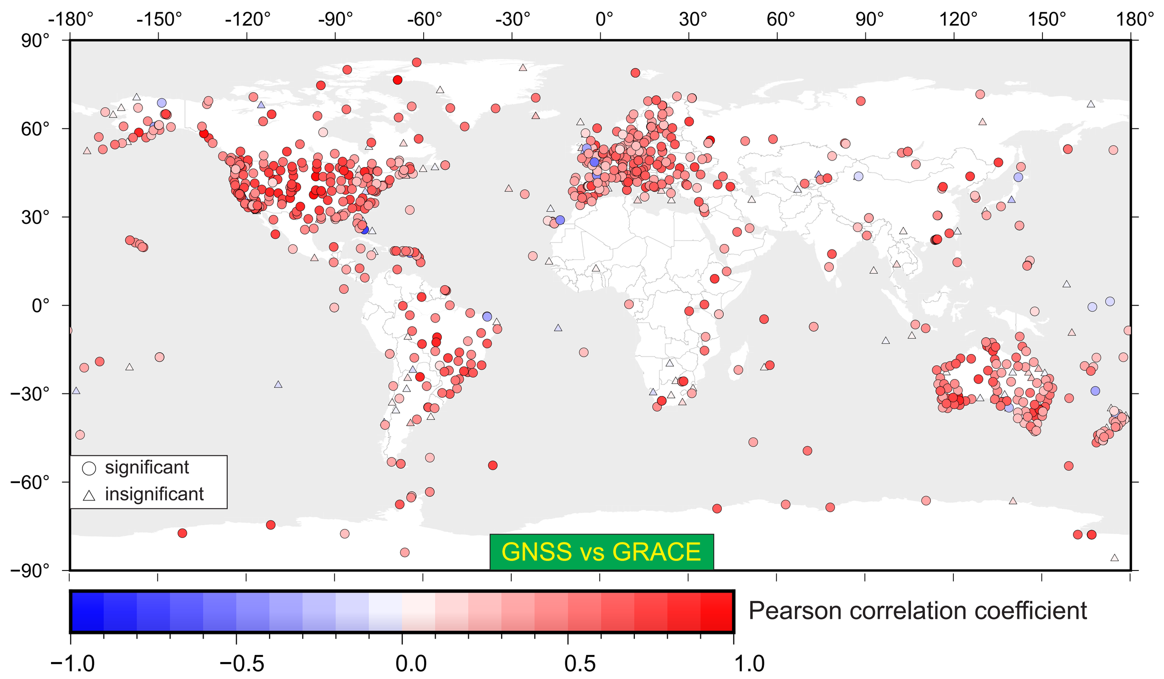

⬆ **Fig. 3.** Pearson correlation coefficients between GNSS (NTAL/NTOL removal) and GRACE after GAC/GAD products restoration and NTAL/NTOL models removal.

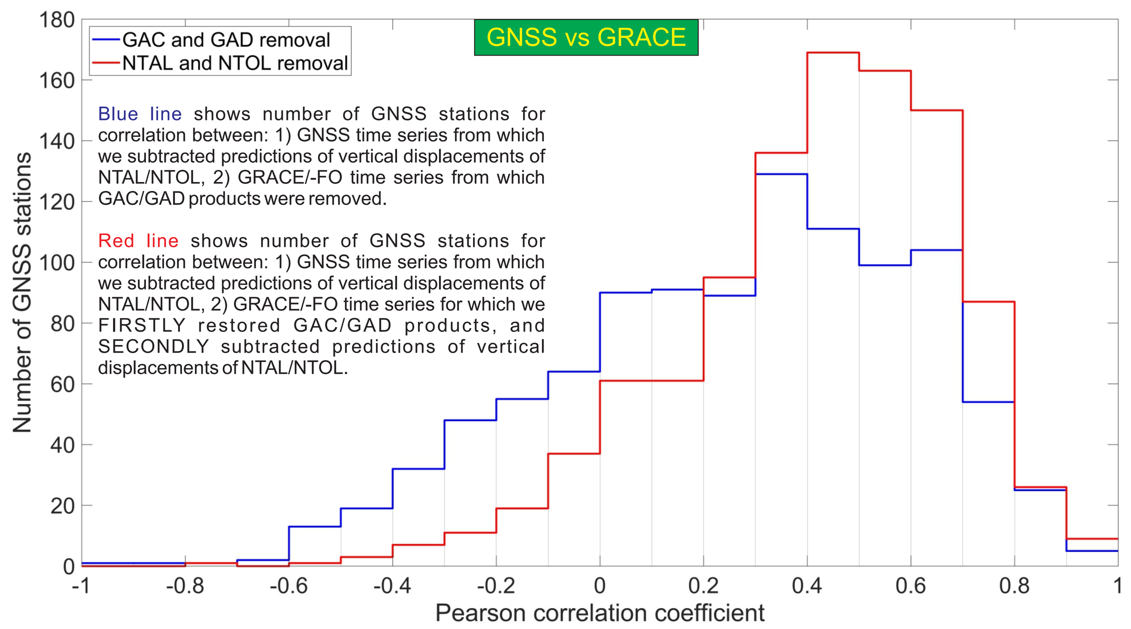

⬆ **Fig. 4.** Histograms of Pearson correlation coefficients between GNSS (NTAL/NTOL removal) and GRACE, when removed from GRACE time series: **1)** GAC and GAD products (blue curve), **2)** NTAL and NTOL models (red curve).

USA 2012 DROUGHT DETECTION

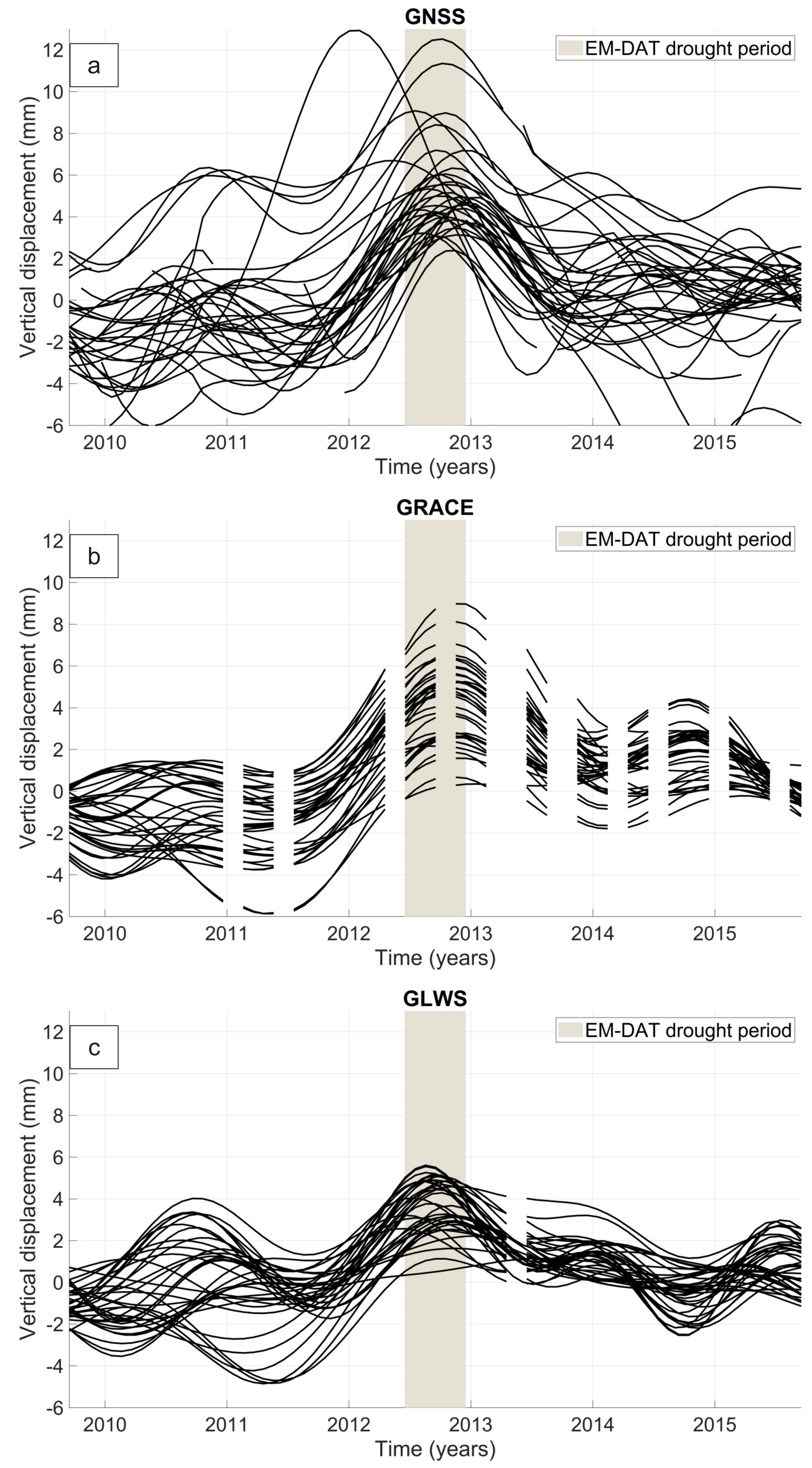

⬆ **Fig. 6.** Chosen GNSS (NTAL/NTOL removal), GRACE (after GAC/GAD products restoration and NTAL/NTOL models removal) and GLWS time series showing the 2012 drought in the United States: **a)** GNSS, **b)** GRACE, **c)** GLWS.

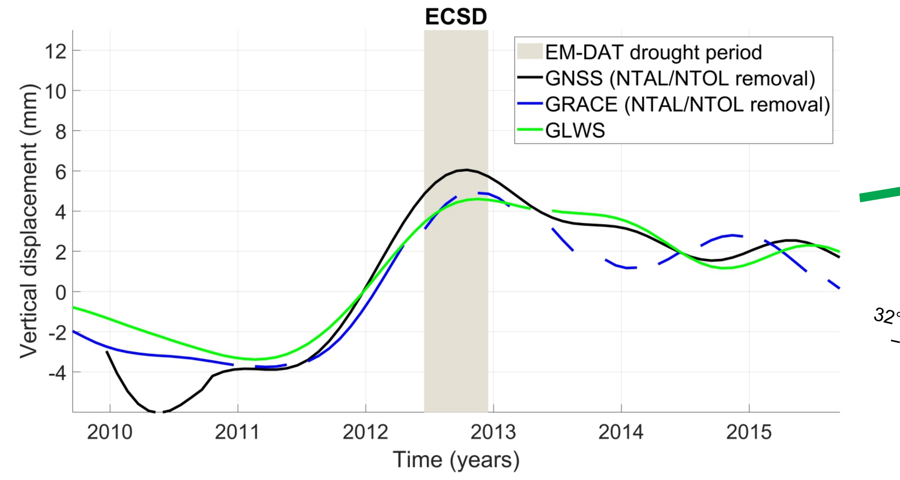

⬆ **Fig. 7.** GNSS (NTAL/NTOL removal), GRACE (after GAC/GAD products restoration and NTAL/NTOL models removal) and GLWS time series showing the 2012 drought in the United States for coordinates of ECSD station.

⬇ **Tab. 1.** Calculated values of the chosen GNSS (NTAL/NTOL removal), GRACE (after GAC/GAD products restoration and NTAL/NTOL models removal) and GLWS time series for the 2012 drought in the United States: **1)** month of the greatest vertical displacement, **2)** value of the greatest vertical displacement, **3)** RMS from the entire time series, **4)** correlations between GNSS and GRACE, as well as GNSS and GLWS.

Acronym	GNSS			GRACE			GLWS			Correlation	
	Peak month	Peak value [mm]	RMS [mm]	Peak month	Peak value [mm]	RMS [mm]	Peak month	Peak value [mm]	RMS [mm]	GNSS vs GRACE	GNSS vs GLWS
ADRI	Nov. 2012	6.3	2.1	Nov. 2012	6.0	2.0	Nov. 2012	3.7	1.3	0.68	0.70
ALGO	Nov. 2012	3.9	1.4	Oct. 2012	4.0	1.4	Sept. 2012	4.9	1.7	0.62	0.56
BSMK	Dec. 2012	7.2	2.5	Nov. 2012	1.9	2.3	Nov. 2012	2.5	1.6	0.54	0.53
★ECSD	Oct. 2012	6.1	3.1	Nov. 2012	4.9	2.2	Nov. 2012	4.6	2.1	0.92	0.94
GODN	Nov. 2012	2.4	1.4	Oct. 2012	2.4	1.1	Nov. 2012	2.9	1.7	0.44	0.61
HOLP	Feb. 2012	12.9	7.8	Jul. 2011	-2.5	1.2	Jun. 2013	1.1	0.8	-0.37	-0.01
HRST	Jul. 2012	9.1	5.9	Nov. 2012	2.8	1.0	Jun. 2013	-0.1	1.9	0.39	0.39
KA14	Sept. 2012	4.2	2.1	Oct. 2012	4.8	1.7	Aug. 2012	3.8	1.2	0.37	0.44
KSU1	Sept. 2012	5.0	2.4	Jan. 2013	5.3	2.3	Oct. 2012	4.9	1.8	0.89	0.79
KUUJ	May 2012	6.7	4.0	Aug. 2012	2.2	1.0	Jan. 2013	2.2	1.2	0.64	0.34
LCDT	Nov. 2012	5.2	2.2	Nov. 2012	6.5	2.1	Oct. 2012	4.3	1.3	0.59	0.58
LCUR	Dec. 2012	4.7	3.0	Nov. 2012	6.4	2.2	Aug. 2012	5.6	1.9	0.19	0.35
LOYF	Sept. 2012	3.1	1.6	Oct. 2012	2.4	1.1	Nov. 2012	3.0	1.7	0.25	0.15
MCHN	Sept. 2012	4.2	1.5	Nov. 2012	4.6	1.8	Jul. 2012	4.0	1.7	0.54	0.52
MIBX	Oct. 2012	9.0	3.1	Oct. 2012	6.3	2.4	Aug. 2012	4.8	1.6	0.61	0.71
MIMQ	Jul. 2012	4.3	2.0	Nov. 2012	7.1	2.6	Aug. 2012	4.9	1.7	0.49	0.61
MNBE	Nov. 2012	3.5	1.4	Nov. 2012	5.3	2.1	Sept. 2012	4.9	2.0	0.64	0.50
MNCA	Oct. 2012	4.0	1.5	Nov. 2012	5.9	2.2	Aug. 2012	5.3	1.6	0.67	0.82
MNRT	Sept. 2012	4.5	2.0	Nov. 2012	3.6	1.9	Oct. 2012	3.3	2.0	0.81	0.87
MNTF	Aug. 2012	4.1	1.8	Nov. 2012	2.7	1.8	Sept. 2012	2.5	1.8	0.75	0.55
MONE	Dec. 2012	4.4	1.8	Nov. 2012	5.2	2.1	Sept. 2012	4.5	1.9	0.73	0.61
MOWR	Aug. 2012	3.2	1.6	Oct. 2012	5.0	1.9	Sept. 2012	5.1	1.8	0.68	0.84
NDMB	Dec. 2012	3.7	2.2	Nov. 2012	0.7	2.3	May 2011	-4.7	1.8	0.61	0.57
NIST	Nov. 2012	5.7	2.4	Jul. 2011	-3.1	1.6	Nov. 2012	3.2	1.1	0.91	0.68
NLIB	Oct. 2012	6.0	2.0	Nov. 2012	5.6	2.1	Sept. 2012	5.2	1.7	0.65	0.66
NOR1	Oct. 2012	11.4	4.6	Nov. 2012	9.0	3.1	Oct. 2012	4.7	1.8	0.85	0.74
P012	Nov. 2012	3.1	1.3	Jul. 2011	-2.8	1.4	Nov. 2012	1.6	0.9	0.81	0.81
PARY	Sept. 2012	8.4	2.9	Nov. 2012	5.6	1.9	Aug. 2012	5.6	1.9	0.88	0.63
PLTC	Jan. 2013	4.9	2.3	Jul. 2011	-3.1	1.6	Nov. 2012	3.1	1.1	0.72	0.74
ROSS	Oct. 2012	5.6	2.5	Oct. 2012	3.7	1.5	Nov. 2014	-2.2	1.6	0.74	0.75
SUP2	Oct. 2012	12.5	4.6	Nov. 2012	8.1	2.9	Sept. 2012	4.5	1.6	0.85	0.78
USNO	Aug. 2012	5.3	1.8	Oct. 2012	2.4	1.1	Nov. 2012	2.8	1.6	0.42	0.53
WIS5	Dec. 2012	4.6	1.7	Oct. 2012	4.5	2.0	Jul. 2012	3.1	1.4	0.71	0.46
WYLC	Dec. 2012	4.9	1.6	Jul. 2011	-3.6	1.7	Oct. 2012	3.2	1.1	0.74	0.78
ZKC1	Sept. 2012	7.2	2.9	Nov. 2012	5.2	2.2	Oct. 2012	5.1	1.9	0.81	0.84

Unfavourable weather conditions over the North Atlantic Ocean, as well as polar jet streams pushed winter storms away towards Canada. Insufficient precipitation and extreme temperature caused severe drought, enhanced by La Niña phenomenon. July 2012 was the second hottest month in USA of all time, resulting in the driest summer since 1988 (Rippey, 2015).

According to EM-DAT database, drought started in **July 2012** and ended in **December 2012**.

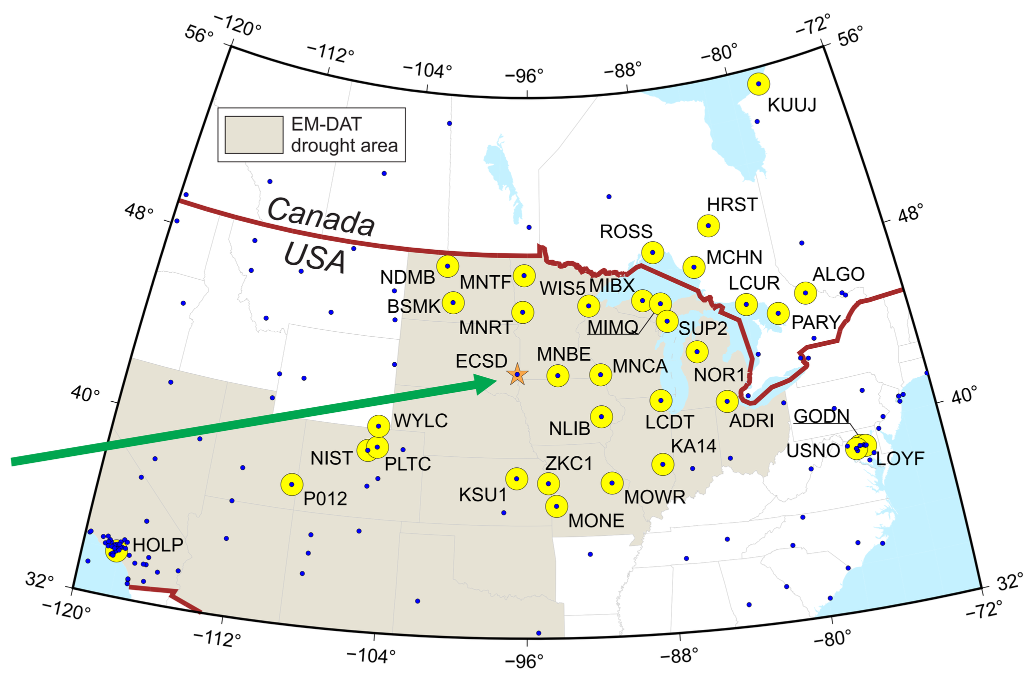

⬆ **Fig. 8.** Distribution of GNSS stations (blue circles) against the background of USA drought in 2012. Stations chosen for analysis of USA drought in 2012 are highlighted with yellow circles (ECSD station with orange star) and have their acronyms assigned.

LONG-TERM SIGNALS OBSERVED USING LOMB-SCARGLE ALGORITHM

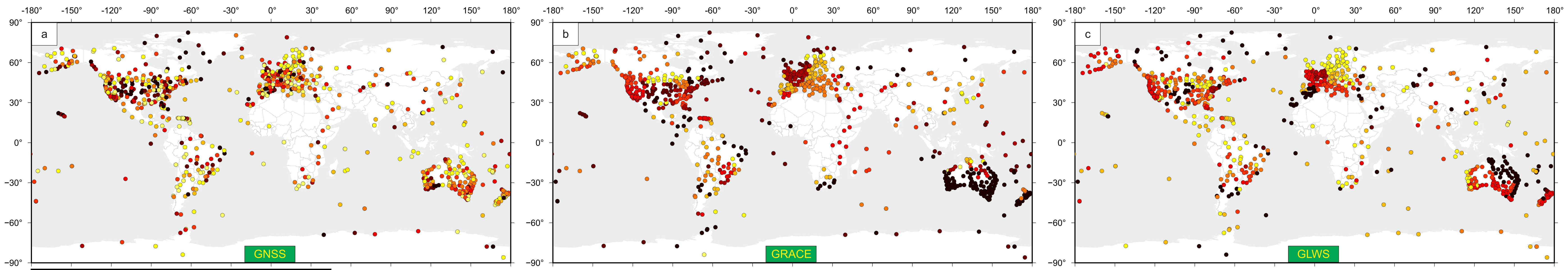

⬉⬆ **Fig. 5.** Periods of signals (years) for maximum power spectral density values (mm^2/Hz), assuming that periods are shorter than 10 years: **a)** GNSS (NTAL/NTOL removal), **b)** GRACE after GAC/GAD products restoration and NTAL/NTOL models removal, **c)** GLWS.

SUMMARY AND CONCLUSIONS

1) Dynamic time warping may lengthen or shorten particular time series, thus we don't get correlation for corresponding epochs. DTW shows completely different results than Pearson correlation method.
2) When removing non-hydrospheric effects from time series, the same models should be used. GAC/GAD products restoration and NTAL/NTOL models removal from GRACE time series improved correlation with GNSS time series after NTAL/NTOL models removal. As a result, number of total well or very well positively correlated GNSS stations (0.7-1.0 coefficients) increased from 84 to 122.
3) Lomb-Scargle algorithm helps in finding periodic signals for unevenly-spaced data sets. Thus, it's really useful in analyses of geodetic time series, which contain epochs of missing values. Signals of long periods were particularly seen in Australia, but also occurred in other parts of the world.
4) Showing the example of the 2012 drought in the United States, it's clear that GNSS technique can be used to study changes in the terrestrial hydrosphere.

REFERENCES

1) Gerdener H., Kusche J., Schulze K., Doll P., Klos A. (**2022**). *The global land water storage data set release 2 (GLWS2.0) derived via assimilating GRACE and GRACE-FO data into a global hydrological model*, (preprint). **DOI:** 10.48550/arXiv.2211.17138.
2) Paliwal K. K., Agarwal A., Sinha S. S. (**1982**). *A modification over Sakoe and Chiba's dynamic time warping algorithm for isolated word recognition*, Signal Processing, 4(4), pp. 329-333. **DOI:** 10.1016/0165-1684(82)90009-3.
3) Rippey B. R. (**2015**). *The U.S. drought of 2012*, Weather and Climate Extremes, 10(A), pp. 57-64. **DOI:** 10.1016/j.wace.2015.10.004.
4) Sakoe H., Chiba S. (**1978**). *Dynamic programming algorithm optimization for spoken word recognition*, IEEE Transactions on Acoustics, Speech, and Signal Processing, 26(1), pp. 43-49. **DOI:** 10.1109/TASSP.1978.1163055.

ACKNOWLEDGEMENTS

This research is financed by the National Science Centre, Poland, grant no. UMO-2021/41/B/ST10/01458.